International Journal of Heat and Mass Transfer 52 (2009) 702–708

Contents lists available at ScienceDirect

International Journal of Heat and Mass Transfer

journal homepage: www.elsevier.com/locate/ijhmt

Approximate solutions of lean premixed combustion in porous media with reciprocating flow

Jun-Rui Shi [a,*], Mao-Zhao Xie [b], Gang Li [c], Hong Liu [b], Ji-Tang Liu [a], Hong-Tao Li [a]

[a] Shenyang Key Laboratory on Circulating Fluidized Bed Combustion Technology, Shenyang Institute of Engineering, Shenyang 110136, China
[b] School of Energy and Power Engineering, Dalian University of Technology, Dalian 116024, China
[c] Civil and Architecture Engineering College, Dalian University, Dalian 116622, China

ARTICLE INFO

Article history:
Received 30 January 2008
Received in revised form 31 July 2008
Available online 22 September 2008

Keywords:
Premixed combustion
Reciprocating flow
Flammability limit
Approximate solution

ABSTRACT

Based on the analogy with the steady countercurrent reactor, a simplified theoretical solution is presented, which is applicable to adiabatic inert porous media combustors with reciprocating flow. The model consists of two ordinary differential equations that link all major controlling parameters, which allow for a good physical understanding of the process. The maximum temperatures in the burner predicted by the simplified model show the same trends as those in experimental results, but are generally higher, and the discrepancy between the experimental data and predications is less than 20%. By analyzing experimental and simulation results, a simplified theoretical solution for the temperature profile in the burner is further developed, which is expressed in terms of a piecewise linear function and the lean flammability limit is presented by a implicit expression. Results show that the lean flammability limit can be extended by using porous media of smaller pore size. The predicted lean flammability limit provides guidelines for the design of the combustor and some indications for further improving the combustor performances.

© 2008 Elsevier Ltd. All rights reserved.

1. Introduction

Premixed combustion in inert porous media draws constant interest of researchers due to its wide applications and outstanding features of pollution control and energy recovery. The research on this issue has been reported extensively in the literature including experimental [1–6], analytical [2,7–11] and numerical studies [12–16]. Howell [17] presented a detailed review of this subject. Recent advance and remaining questions in this area were summarized and reviewed by Kamal and Mohamad [18].

Borrowing energy from premixed flame to preheat the incoming reactants, since introduced by Weinberg [7], has been investigated by numerous researchers to clarify the mechanism of heat recirculation [1,8,9]. The effect of this recuperation leads to a local temperature in excess of the adiabatic flame temperature. Thus, the flammability limits can be extended to some extent. Zhdanok et al. [2] experimentally and theoretically studied the superadiabatic combustion in packing bed and stable combustion was observed for methane/air mixtures with an equivalence ratio of 0.15. However, further extensions of the range of lean flammability were limited under this condition.

To deal with ultra-lean gas mixtures without external energy supplied, reciprocating superadiabatic combustion of premixed gases in inert porous media (RSCP) was proposed, in which the direction of the flow was periodically changed at a regular interval. Through the reciprocating flow, heat stored in the hot zone can always be used for preheating the fresh mixture and thus the flammability limits were successfully extended. Hoffmann et al. [3] experimentally studied the behavior of a RSCP system and the combustible limit was extended to an extremely low equivalence ratio of 0.026 for methane/air mixture. Good performance regarding emission characteristics was also observed in their experiment. Subsequently, an improved structure with a center space for RSCP was proposed by Hoffmann et al. [13]. Results showed that the new arrangement of the porous media could stabilize flame position for a wide operating range and largely extend the flammability range. Recently, Dobrego et al. investigated lean combustibility limit for RSCP using analytical and numerical methods [19]. In their study, particular attention was focused on the influence of practically important parameters (heat loss coefficient, reactor length, pressure, particles size, porosity) on the lean combustibility limit.

In the predictions by Hanamura et al. [14] for combustion in RSCP, the flame temperature in porous media is 13 times higher than the theoretical one of the conventional open flame. The heating value of the combustible gas is about 65 KJ m^{-3}, which is equivalent to a temperature increase of only 50 K.

RSCP system has shown the best combustion enhancement performance in various applications, including burning ultra-lean mixture [20], regeneration process [23], fuel reforming [21,22]

* Corresponding author. Tel.: +86 24 31975539.
E-mail address: shijunrui2002@163.com (J.-R. Shi).

0017-9310/$ - see front matter © 2008 Elsevier Ltd. All rights reserved.
doi:10.1016/j.ijheatmasstransfer.2008.08.002

Nomenclature

A	pre-exponential factor
c	specific heat
E	activation energy
h_0	low heating value
h_v	convective heat factor
L	combustor length
R	universal gas constant
Y	mass fraction
T	temperature
T_0	ambient temperature
T_{ad}	adiabatic temperature
T_{ign}	ignition temperature
T_{max}	maximum temperature
u_g	gas velocity
W	reaction rate

Greek symbols

φ	equivalence ratio
λ_{se}	effective thermal conductivity
ρ	density
γ	mass fraction of fuel in the unburned stream
ε	porosity
ω	thermal front speed
τ	reverse time period

Subscripts

g	gas
g2	gas flow 2
e	burner exit
g1	gas flow 1
s	solid

and heat extract [4–6]. The system has been successfully applied to burning of the organic pollutants in exhaust air from paint spray boxes in car factories [20]. Based on the heat recovery properties of RSCP, Konstandopoulos and Kostoglou [23] studied its applications for the improvement of the regeneration process of diesel particulate filters. The numerical results confirmed the capability of the new technique to provide a clean filter for applications where conventional regeneration failed. Researches on heat extract from RSCP system with embedded heat exchangers have appeared and concentrated on the thermal efficiency and pollutant emissions [4–6]. It was shown that the heat extraction efficiency increased from 70% to 80%, as the equivalence ratio increased in the range $0.1 < \varphi < 1.0$ and that the pollutant emissions were very low [4].

Similarly, for the sake of treatment of lean mixtures of waste gases the catalytical reverse-flow reactors have been deeply investigated in the past 30 years [24]. Nieken et al. [25] analyzed two limiting cases of very large and very short switching periods. Through simplifying a pseudo-homogeneous model, they presented simple quasi-analytical expressions for most important parameter profiles. Subsequently, this model was further developed by Cittadini et al. and limiting operating conditions could be predicted [26].

As shown in the previous studies on RSCP, the characteristic of this system has been mostly studied through experiments [3,4] and numerical calculations [13–15]. Theoretical analysis on RSCP characteristic, such as the maximum temperature, temperature gradient and combustible limits is not yet available, which is very important to physically understand the nature of this system and for burner design.

The specific objectives of this paper is to present a simplified analytical solution for the RSCP system. The study includes the following contents: (i) based on the analogy with the steady countercurrent reactor, a simple model is conducted; (ii) a temperature distribution function in the burner for lean premixtures is constructed; (iii) an implicit expression for the lean combustible limit of burner is obtained. Finally, the influence of different porous media on flammability limit is discussed.

2. Mathematical model

2.1. Complete model

In a previous study, Nieken et al. [25] have presented a detailed analogy analysis for catalytic reverse-flow combustor. However, in our model, catalytic effect is negligible and the basic equations differ with those of Nieken et al. To distinctly clarify the problem and for later analysis, the analogy process for RSCP is performed in this study. Our original contribution consists of a further development of the investigation by Nieken et al. [25], in order to construct the temperature distribution and present an implicit expression of flammability limit for RSCP and so on.

The model arises from the analogy between the high switching frequency RSCP and a steady countercurrent reactor. Fig. 1a and b show the sketch of the countercurrent reactor and temperature profiles inside it. For the latter one, one of two flows is sent in one direction and the other is simultaneously in the opposite direction. Through the solid phase, the cold inlet flow is heated by the hot outlet flow. The analogy between the two systems is based on the fact that they have the essential phenomenon in common, even though they have different behaviors in operation, such as a pseudo-steady and a direct heating between phases. For RSCP, a direct heating occurs between the two phases and a pseudo-steady state is reached after several reversal time period. If the frequency is very high, the solid temperature will not change due to its relatively high thermal capacity, while the gas temperatures fluctuate between the two profiles below or above the solid temperature during every half cycle. Although the two systems are different in operation, the behaviors of the two burners are very similar

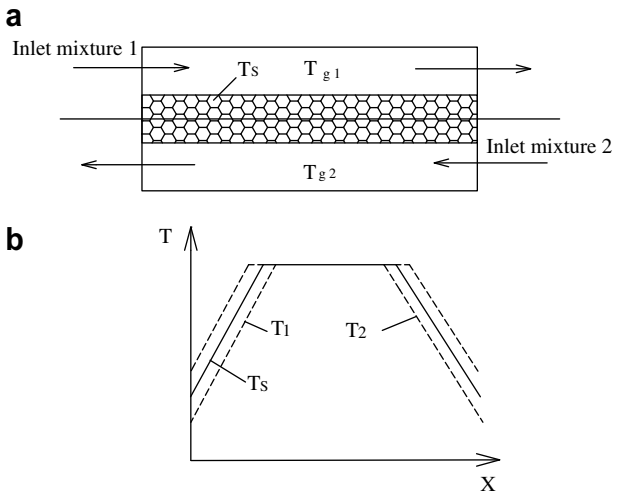

Fig. 1. (a) Sketch of the countercurrent reactor. (b) Temperature profiles of countercurrent reactor.

and the model assembled for the countercurrent reactor can be used for the RSCP.

For simplicity we introduce the following assumptions:

(1) Porous media filled in the combustor are noncatalytic, homogeneous and optically thick. The solid radiation is taken into account by using the Rosseland approximation.
(2) Gas flow in porous media is laminar and pressure lose in the burner is neglected.

Under the above assumptions, a set of differential equations can be obtained.

Solid energy equation

$$(1-\varepsilon)\lambda_{se}\frac{d^2T_s}{dx^2}+\frac{1}{2}h_v(T_{g1}-T_s)+\frac{1}{2}h_v(T_{g2}-T_s)=0 \tag{1}$$

where T_{g1}, T_{g2}, are gas temperature of flow 1 and 2, respectively; T_s, solid phases temperature; ε porosity; h_v, convective heat factor; λ_{se} is effective thermal conductivity of the porous media, which includes the influence of radiation by Rosseland approximation, assuming an optically thick region around the high temperature zone in the bed.

Energy equation of gas phase 1 and 2

$$-\varepsilon\rho_g u_g c_g\frac{dT_{g1}}{dx}+\varepsilon\lambda_g\frac{d^2T_{g1}}{dx^2}-h_v(T_{g1}-T_s)+h_0\varepsilon\gamma W_{g1}=0 \tag{2}$$

$$\varepsilon\rho_g u_g c_g\frac{dT_{g2}}{dx}+\varepsilon\lambda_g\frac{d^2T_{g2}}{dx^2}-h_v(T_{g2}-T_s)+h_0\varepsilon\gamma W_{g2}=0 \tag{3}$$

W_{g1}, W_{g2} are methane reaction rate for flow 1 and 2, respectively; h_0, low heating value of fuel; λ_g, gas thermal conductivity; γ, mass fraction of fuel in the unburned stream.

Species conservation equation for gas phase 1 and 2

$$-\rho_g u_g\frac{dY_{g1}}{dx}+D\frac{d^2Y_{g1}}{dx^2}+W_{g1}=0 \tag{4}$$

$$\rho_g u_g\frac{dY_{g2}}{dx}+D\frac{d^2Y_{g2}}{dx^2}+W_{g2}=0 \tag{5}$$

The reaction rate of methane is described by a single-step first-order Arrhenius type expression [15]

$$W_{g1}=\rho_{g1}Y_{g1}Ae^{-E/(RT_{g1})} \tag{6}$$

$$W_{g2}=\rho_{g2}Y_{g2}Ae^{-E/(RT_{g2})} \tag{7}$$

where E, activation energy; R, universal gas constant; A, pre-exponential factor.

2.2. Simplified model

2.2.1. The maximum temperature and temperature gradient

To simplify the problem, the following assumptions were introduced:

(1) The physical properties of solid and gas phases are constant.
(2) The diffusion effect of species in the gas mixtures is not considered. That is to say, the second terms are neglected in Eqs. (4) and (5).
(3) The gas phase conductivity is very small in comparison with that of the solid and, hence, not considered. In other words, the second terms are neglected in Eqs. (2) and (3).

Combining Eq. (1) with (2) and (3), we obtain

$$2(1-\varepsilon)\lambda_{se}\frac{d^2T_s}{dx^2}+\varepsilon\rho_g u_g c_g\left(\frac{dT_{g2}}{dx}-\frac{dT_{g1}}{dx}\right)+h_0\varepsilon\gamma(W_{g1}+W_{g2})=0 \tag{8}$$

Subtracting Eqs. (2) and (3), then after differentiation, we get

$$\varepsilon\rho_g u_g c_g\left(\frac{dT_{g2}}{dx}-\frac{dT_{g1}}{dx}\right)-\frac{h_0\gamma\rho_g u_g c_g\varepsilon^2}{h_v}(W_{g2}-W_{g1})' =\frac{(\varepsilon\rho_g u_g c_g)^2}{h_p}\left(\frac{d^2T_{g2}}{dx^2}+\frac{d^2T_{g1}}{d^2x}\right) \tag{9}$$

T_s could be approximated by the expression

$$T_s=\frac{T_{g1}+T_{g2}}{2} \tag{10}$$

Substituting Eq. (10) into (9) yields

$$2\lambda_{eff}\frac{d^2T_s}{dx^2}+\frac{h_0\gamma\rho_g u_g c_g\varepsilon^2(W_{g2}-W_{g1})'}{h_v}+h_0\gamma\varepsilon(W_{g2}+W_{g1})=0 \tag{11}$$

where

$$\lambda_{eff}=(1-\varepsilon)\lambda_{se}+\frac{(\varepsilon\rho_g u_g c_g)^2}{h_v} \tag{12}$$

$$(W_{g2}-W_{g1})'=-\rho_g u_g\left(\frac{dY_{g2}}{dx}+\frac{dY_{g1}}{dx}\right)' \tag{13}$$

$$(W_{g2}+W_{g1})=-\rho_g u_g\left(\frac{dY_{g2}}{dx}-\frac{dY_{g1}}{dx}\right) \tag{14}$$

Substituting Eqs. (13) and (14) into (11) and integrating yields

$$2\lambda_{eff}\frac{dT_s}{dx}-h_0\gamma\varepsilon\rho_g u_g(Y_{g2}-Y_{g1})=\frac{h_0\gamma c_g(\varepsilon\rho_g u_g)^2\left(\frac{dY_{g2}}{dx}+\frac{dY_{g1}}{dx}\right)}{h_v} \tag{15}$$

To obtain the maximum temperature expression, we assume that full conversion is reached in the middle of the reactor. Thus, we get

$$\frac{dY_{g2}}{dx}=Y_{g2}=0$$

Thus, Eq. (15) can be reduced to

$$2\lambda_{eff}\frac{dT_s}{dx}+h_0\gamma\varepsilon\rho_g u_g Y_{g1}=\left[h_0\gamma c_g(\varepsilon\rho_g u_g)^2\frac{dY_{g1}}{dx}\right]\Big/h_v \tag{16}$$

Substituting Eq. (4) into Eq. (16), we obtain

$$\frac{dT_s}{dx}=\left(F-Ge^{\frac{E}{RT_s}}\right)\frac{dY_{g1}}{dx} \tag{17}$$

where $F=\frac{h_0\gamma c_g(\varepsilon\rho_g u_g)^2}{2\lambda_{eff}h_v}$, $G=-\frac{h_0\gamma\varepsilon\rho_g u_g^2}{2\lambda_{eff}A}$

Boundary conditions for Eq. (17) are [26].

At the burner inlet

$$T|_{X=0}=T^0+\frac{\Delta T_{ad}}{2}\left(1-\frac{Y^e}{Y^0}\right),\quad Y_1|_{X=0}=Y^0=1,\quad Y_2|_{X=0}=Y^e \tag{18}$$

At the point of symmetry in the middle of the reactor

$$Y_1|_{X=L/2}=Y_2|_{X=\grave{o}/2} \tag{19}$$

Integrating Eq. (17) from $x=0$ to $x=L/2$ with boundary conditions (Eqs. (18) and (19)) yields

$$\int_{T_0+\frac{1}{2}\Delta T_{ad}}^{T_{max}}\frac{1}{Ge^{\frac{E}{RT_s}}-F}dT_s=Y_0-Y_e=Y_0=1 \tag{20}$$

Eq. (20) gives an implicit expression for the maximum temperature in the burner and it can be easily solved with a short computer code. To evaluate the temperature slopes of the preheating zone, we neglect chemical reaction in this zone, deriving the following analytical expression

$$\frac{dT_s}{dx}=\frac{h_0\gamma\varepsilon\rho_g u_g Y_0}{2\lambda_{eff}} \tag{21}$$

The complete model now is simplified to only two ordinary differential equations (Eqs. (20) and (21)). As shown in Eqs. (20) and (21), T_{max} and dT_s/dx are independent from the half cycle, in agreement with the experimental results of Hoffmann et al. [3].

2.2.2. Effect of mixture velocity and equivalence ratio on T_{max}

Fig. 2a shows effect of equivalence ratio on T_{max} for three different mixture velocities. As expected, increasing equivalence ratio leads to an increase in T_{max}. Results show that equivalence ratio has significant effect on T_{max}. Qualitative agreement between the theoretical model and experiment [3] can be noted, but the predictions are generally higher, and the deviation between the theoretical solution and experimental data is less than 20% for the calculation equivalence ratio range of 0.03–0.3. Insight on the reason for the discrepancy can be obtained by an examination of the model used in this study. Since the adiabatic boundary is adopted in the model, it is understandable that the theoretically predicted T_{max} exceeds the experimental value. This may be one of main reasons for the discrepancy. Another reason may be attributed to the uncertainties in the thermal properties of the packed bed as well as to the global methane oxidation mechanism. Further, it is noted that natural gas used in the experiment (88% methane and other species) differs with that in the theoretical analysis (100% methane). Fig. 2b depicts that mixture velocity has significant influence on maximum temperature.

2.2.3. Construction of temperature profile

As shown in earlier numerical work [14], reciprocating filtration combustion typically exhibits a flatter temperature plateau in the central region of the reciprocating combustor when heat loss is neglected. The temperature profile has a typical trapezoidal shape. In fact, heat loss through burner walls to the surroundings is inevitable and this leads to a minimum temperature at the reactor midpoint [3,15]. However, in this work the heat loss is not taken into account and we construct the temperature profile in terms of trapezoidal shape.

Hoffmann et al. [3] experimentally observed that the high temperature zone propagated at an almost constant speed from the upstream side of the burner towards the downstream end during a half cycle. During this process, the temperature gradients at both the upstream and downstream ends traveled nearly in parallel. This transient characteristic of RSCP indicates that the temperature profile at the end of the half cycle is just the one at the beginning of the half cycle, which shifts downstream with the flow. The travel distance corresponds to $\omega\tau$. Thus, we get

$$T_{s0} - T_{out} = \omega\tau \frac{dT_s}{dx} \tag{22}$$

where T_{so}, T_{out} are solid temperatures at the beginning and end of half cycle; τ is the half cycle. The velocity of the moving thermal front can be approximated by Matros [24]

$$\omega = \frac{c_g \rho_g u_g}{c_s \rho_s (1-\varepsilon)} \left(1 - \frac{\Delta T_{ad}}{T_{max} - T_0}\right) \tag{23}$$

Fig. 3 presents the temperature profile constructed by a piecewise linear function. The temperature gradients at the burner inlet and outlet can be obtained from Eq. (21). Eq. (20) presents the maximum temperature in the burner. As it stands, both the inlet and outlet temperature in the burner are not yet known. However, the main purpose of using the RSCP is to expand the lean flammability limit, which is situation in this work. Experimental and numerical simulation works indicate that T_{so} can be approximated by T_0 at the end of the half cycle under this condition [3,14]. Substituting T_0 into Eq. (22) yields

$$T_{s0} - T_0 = \omega\tau \frac{dT_s}{dx} \tag{24}$$

As shown in Fig. 4, the combustor length L is described as

$$L = \frac{T_{ign} - T_{s0}}{dT_s/dx} + L_{hz} + \frac{T_{ign} - T_{out}}{dT_s/dx} \tag{25}$$

where L_{hz} is the length of the center hot zone. For simplification, the ignition temperature for methane is empirically given as [27]

$$T_{ign} = 0.75 T_{max} \tag{26}$$

Fig. 4 shows comparisons of analytically predicted temperature with experimental results for three different operation conditions. Ceramic foam with a same porosity (0.875) but different pore size was used in Fig. 4 (13 ppi for Fig. 4a and c, 30 ppi for Fig. 4b, respectively). Results show that porous media used in the burner have significant influence on the RSCP performance. Wider hot zone and higher maximum temperature for smaller pore size (30 ppi) are

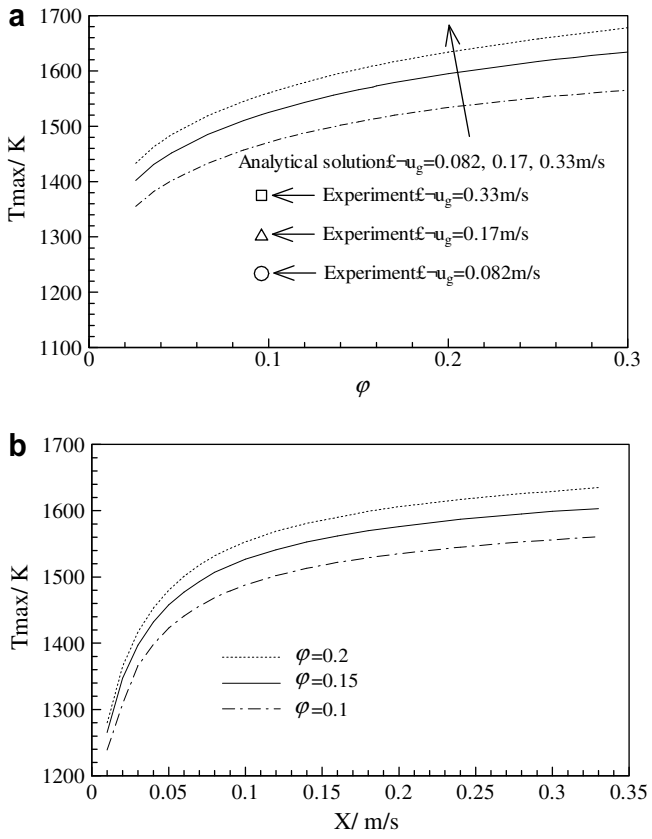

Fig. 2. Effect of operation parameters on the T_{max} (13 ppi). (a) Equivalence ratio. (b) Mixture velocity.

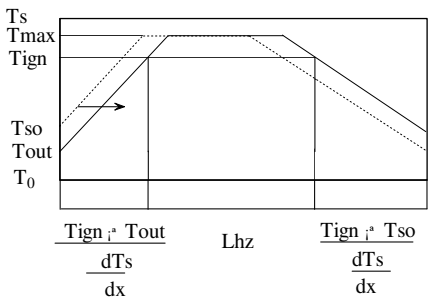

Fig. 3. Construction of the temperature profile at the end (solid line) and beginning of the cycle (dashed line).

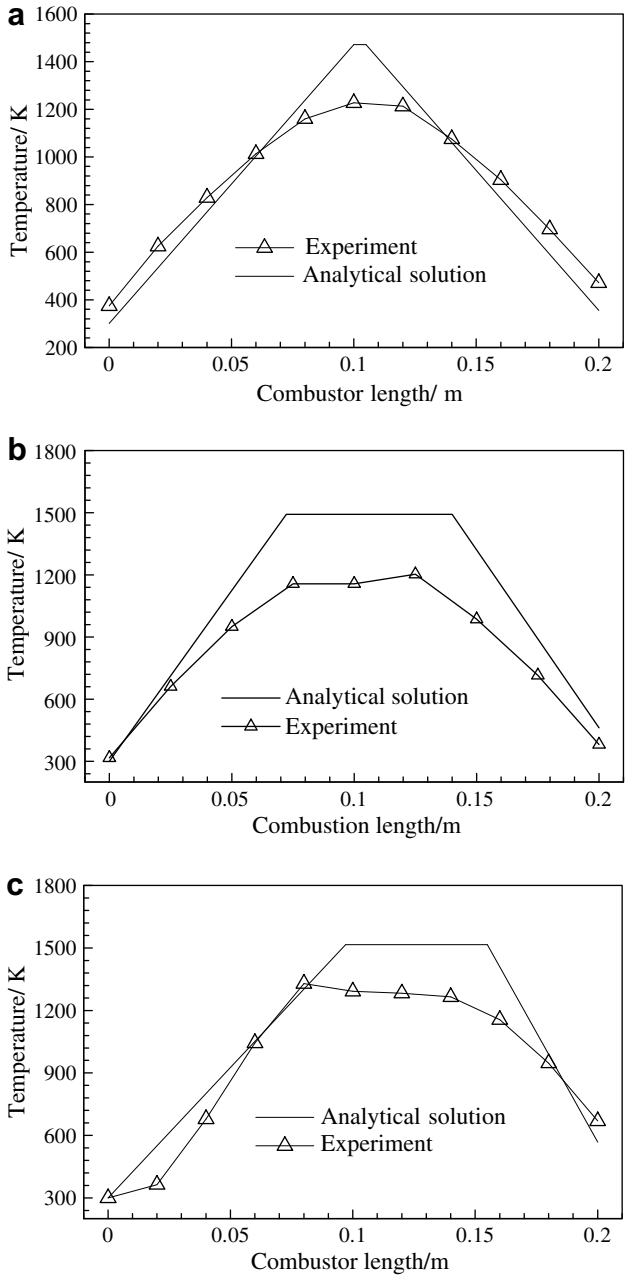

Fig. 4. Comparison of analytical prediction of the temperature with experimental results. (a) 13 ppi porous media (u_g = 0.083 m/s, φ = 0.1, T_{csp} = 30 s). (b) 30 ppi porous media (u_g = 0.083 m/s, φ = 0.096, T_{csp} = 30 s). (c) 13 ppi porous media (u_g = 0.17 m/s, φ = 0.096, T_{csp} = 90 s).

observed from Fig. 4, although the equivalence ratio in Fig. 4b (φ = 0.1) are greater than that in Fig. 4a (φ = 0.096). To further validate the performance of the simplified model, we conducted a sample calculation (Fig. 4c) in which the product of the flow velocity and reciprocating cycle time is relatively larger. It is clear that obvious displacement towards the downstream is well predicted by the theoretical solution. However, the maximum temperature in the burner is overpredicted as shown in Fig. 4a and b.

To clarify the influence of pore size on RSCP performance, Fig. 5 illustrates the dependence of the maximum temperatures on pore size of the porous media. In the range of $0.05 \leqslant u_g \leqslant 0.3$, the maximum temperatures for smaller pore size (30 ppi) porous media are always greater than that of larger pore size (13 ppi). So we can conclude that, for fuel-lean premixtures, the smaller pore size porous

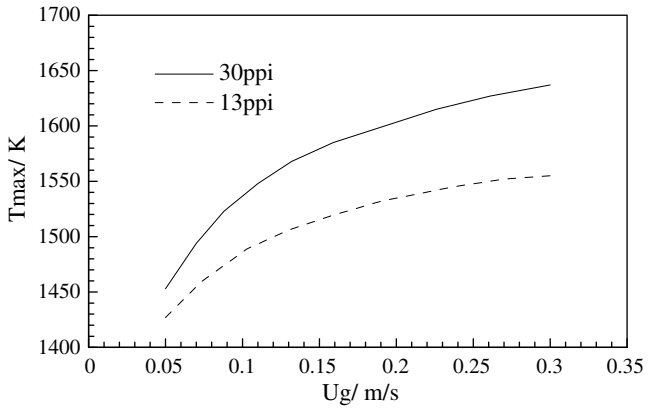

Fig. 5. Effect of inlet velocities on the maximum temperature for two different porous media ($u_g * T_{csp}/L$ = 25, φ = 0.1).

media is advantageous to form higher temperature zone in RSCP burner under certain condition.

The 10 and 30 ppi ceramic foams used here have the same porosity of 0.875 but different pore sizes, this leads to different absorption coefficients and different effective internal volumetric surface areas for convective heat transfer between the porous media and fluid [3]. Porous media with smaller pore size means relatively larger extinction coefficient and this ensures the forming of a local high temperature zone. In additional, smaller pore size leads to more extensive heat transfer between the porous body and gas mixtures, thus the fresh mixture is effectively preheated.

2.2.4. Flammability limit

It is known that the temperature profile in RSCP system has a typical trapezoidal shape. The equivalence ratio mainly affects both the lateral temperature gradients and the width of the central plateau. A high and wide temperature zone in the burner was observed in the experiment with relatively higher equivalence ratios. When the width of central zone is close to zero (L_{hz} = 0), this corresponds roughly to the flammability limit. Substituting the expression L_{hz} = 0 into Eq. (25) yields

$$L - \frac{2T_{max} - 2T_{out}}{dT_s/dx} + \omega T_{au} = 0 \tag{27}$$

Eq. (27) is then the implicit expression for the flammability limit. For given operating parameters and a specified RSCP burner, it is easy to find an equivalence ratio to satisfy Eq. (27). Compared to the complete model, with this procedure an enormous computing time is saved.

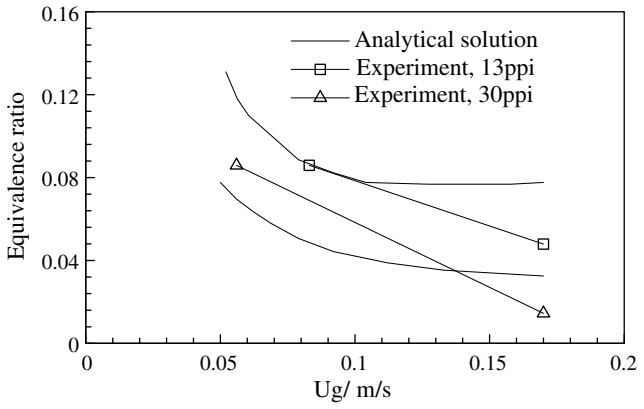

Fig. 6. Comparison of analytical prediction of flammable limit with experimental results ($u_g * T_{csp}/L$ = 25).

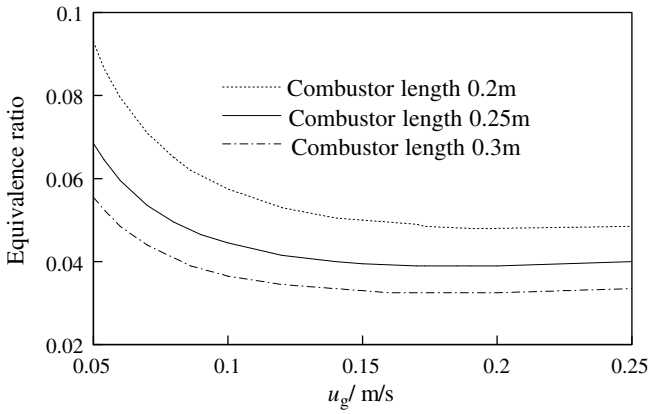

Fig. 7. Effect of inlet velocities on flammable limit for three different combustor length (30 ppi porous media, $u_g * T_{csp} = 5$).

Fig. 6 presents comparison of our theoretically predicted flammability limits with experimental results [3] for 13 and 30 ppi ceramic foams. Both the theoretical and experimental results show that, when u_g is smaller than 0.1 m/s, a steep rise in the flammability limit was observed with increasing u_g. In this case, increasing u_g can overcome a given extinction limit. This indicates that the burner performance can be improved by increasing u_g when ultra-lean mixture is feeded. When u_g is greater than 0.1 m/s, theoretical predictions show the same trend as in the experiment for 30 ppi. However, theoretically predicted results show that u_g has little influence on the flammability limits and this agrees with experimental results. Further, theoretically predicted results show that, in the range of $0.05 \leqslant u_g \leqslant 0.17$, flammability limits can be extended by using smaller pore size porous media.

This discrepancy is probably due to the assumptions used in the model. First, the flow in porous media was assumed to be laminar. In fact, the flow inside the porous media may be turbulent, especially in case of porous media with high porosity and high mixture velocity. Second, the flammability limit expression was obtained only phenomenological by analyzing the temperature profile in literature [3,15], rather than by investigating the extinction mechanism in pore. In addition, as stated previously, the heat loss is neglected. Further research on this subject is required.

As shown in Fig. 7, increasing combustor length extends flammability limit. The longer the combustor, the lower flammability limit can be obtained. However, long porous media lead to an increase in pressure loss and large apparatus. Fig. 7 shows the same trend as experimental data [3]. In their study, both the cross-section and the length of the porous media were increased. As a result, the combustible limit was extended from 0.028 to 0.026.

3. Conclusion

By analogy with the steady countercurrent reactor, a simplified model for RSCP was set up, which consists of only two ordinary differential equations. Based on the model the temperature distribution in the burner was presented in terms of a piecewise linear function. In addition, we deduced an implicit expression for the flammability limit of RSCP. As shows in our analysis, the flammability limit can be extended by increasing inlet mixture velocity and the combustor length as well as by using smaller pore size porous media.

Though a simplified model for RSCP is presented and further developed in this work, detailed experimental study and theoretical analysis are still required. The presented model is useful for initial investigation and qualitative analysis of the RSCP system but should be considered oversimplified for most engineering application. Although no new information (compared to other models or methods) can be obtained by using this model, the model is interesting from the methodological viewpoint, because of using counterflow reactor analogy. Problems, such as species distribution, the influence of heat loss on RSCP performance, remain open. The present model is applicable for smaller inlet gas velocities (say, smaller than 0.1 m/s). To obtain accurate predictions of lean flammability limits, the turbulent effect should be considered when the inlet velocity is greater. We hope that the results of our analysis encourage such investigations.

Acknowledgements

The authors acknowledge the support to this work by the National Natural Science Foundation of China (NSFC Grant Nos. 50076005 and 50476073).

References

[1] D.K. Min, H.D. Shin, Laminar premixed flame stabilized inside a honeycomb ceramic, Int. J. Heat Mass Transfer 34 (2) (1991) 341–356.
[2] S. Zhdanok, L.A. Kennedy, G. Koester, Superadiabatic combustion of methane air mixtures under filtration in a packed bed, Combust. Flame 100 (1995) 221–231.
[3] J.G. Hoffmann, R. Echigo, H. Yoshida, S. Tada, Experimental study on combustion in porous media with a reciprocating flow system, Combust. Flame 111 (1997) 32–46.
[4] F. Contarin, W.M. Barcellos, A.V. Saveliev, et al., Energy extraction from a porous media reciprocal flow burner with embedded heat exchangers, Heat Mass Transfer 127 (2) (2005) 123–130.
[5] S. Jugjai, A. Sawananon, The surface combustor-heater with cyclic flow reversal combustion, Exp. Thermal Fluid Sci. 25 (2001) 183–192.
[6] S. Jugjai, A. Sawananon, The surface combustor-heater with cyclic flow reversal combustion embedded with water tube bank, Fuel 83 (2004) 2369–2379.
[7] F.J. Weinberg, Combustion temperature: the future?, Nature 233 (5317) (1971) 239–241
[8] T. Takeno, K. Sato, A theoretical study on an excess enthalpy flame, in: Eighteen Symposium (International) on Combustion, The Combustion Institute, 1981, pp. 1503–1509.
[9] Y. Yoshizawa, K. Sasaki, B. Echigo, Analytical study of the structure of radiation controlled flame, Int. J. Heat Mass Transfer 31 (2) (1998) 311–319.
[10] S.I. Foutko, S.I. Shabunya, S.A. Zhdanok, Superadiabatic combustion wave in a diluted methane–air mixture under filtration in a packed bed, in: Twenty-Sixth Symposium (International) on Combustion, The Combustion Institute, Naples, 1996, pp. 3377–3382.
[11] V.I. Bubnovich, S.A. Zhdanok, K.V. Dobrego, Analytical study of the combustion waves propagation under filtration of methane–air mixture in a packed bed, Int. J. Heat Mass Transfer 49 (2006) 2578–2586.
[12] M.R. Henneke, J.L. Ellzey, Modeling of filtration combustion in a packed bed, Combust. Flame 117 (1999) 832–840.
[13] J.G. Hoffmann, R. Echigo, S. Tada, Analytical study on flame stabilization in reciprocating combustion in porous media with high thermal conductivity, in: Twenty-Sixth Symposium (International) on Combustion, The Combustion Institute, 1966, pp. 959–966.
[14] K. Hanamura, R. Echigo, Superadiabatic combustion in a porous medium, Int. J. Heat Mass Transfer 36 (13) (1993) 3201–3209.
[15] F. Contarin, A.V. Saveliev, A.A. Fridman, A reciprocal flow filtration combustor with embedded heat exchangers: numerical study, Int. J. Heat Mass Transfer 46 (2003) 949–961.
[16] R.S. Dhamrat, J.L. Ellzey, Numerical and experimental study of the conversion of methane to hydrogen in a porous media reactor, Combust. Flame 144 (2006) 698–709.
[17] J.R. Howell, M.J. Hall, J.L. Ellzey, Combustion of hydrocarbon fuels within porous inert media, Prog. Energy Combust. Sci. 22 (1996) 121–145.
[18] M.M. Kamal, A.A. Mohamad, Combustion in porous media, Proc. ImechE A J. Power Energy 220 (2006) 487–508.
[19] K.V. Dobrego, N.N. Gnesdilov, S.H. Lee, et al., Lean combustibility limit of methane in reciprocal flow filtration combustion, Int. J. Heat Mass Transfer 51 (2008) 2190–2198.
[20] Commercial Report: A New Method of Destroying Organic Pollutants in Exhaust Air, ADTEC Co., Ltd., 1990.
[21] L.A. Kennedy, J.P. Bingue, A. Saveliev, et al., Chemical structures of methane–air filtration combustion waves for fuel-lean and fuel-rich conditions, Proc. Combus. Inst. 28 (2000) 1431–1438.
[22] M. Drayton, A.V. Saveliev, L.A. Kennedy, et al., Syngas production using superadiabatic combustion ultra-rich methane–air mixtures, in: 27th Symposium (International) on Combustion/the Combustion Institute, 1998, pp. 1361–1367.
[23] A.G. Konstandopoulos, M. Kostoglou, Reciprocating flow regeneration of soot filters, Combust. Flame 121 (2000) 488–500.

[24] Y.S. Matros, Forced unsteady-state processes in heterogeneous catalytic reactors, Can. J. Chem. Eng. 74 (1996) 566–579.
[25] U. Nieken, G. Kolios, GAL. Eigenberger, Limiting cases and approximate solution for fixed bed reactors with periodic flowreversal, AIChE J. 41 (8) (1995) 1915–1925.
[26] M. Cittadini, M. Vanni, A.A. Barresi, et al., Simplified procedure for design of catalytic combustors with periodic flow reversal, Chem. Eng. Process. 40 (2001) 255–262.
[27] Irvin Glassman, Combustion [M], third ed., Academic Press, California, USA, 1996.